PEGylation of Nanosubstrates (Titania) with Multifunctional Reagents: At the Crossroads between Nanoparticles and Nanocomposites

ARTICLE *in* LANGMUIR · JULY 2012

Impact Factor: 4.46 · DOI: 10.1021/la3012958 · Source: PubMed

Langmuir

Article

pubs.acs.org/Langmuir

PEGylation of Nanosubstrates (Titania) with Multifunctional Reagents: At the Crossroads between Nanoparticles and Nanocomposites

Tania Kotsokechagia,[†] Noha M. Zaki,[‡,§] Karen Syres,[∥] Piero de Leonardis,[†] Andrew Thomas,[∥] Francesco Cellesi,*[,†] and Nicola Tirelli*[,⊥]

[†]School of Pharmacy and Pharmaceutical Sciences, University of Manchester, Manchester M13 9PT, United Kingdom

[‡]Department of Pharmaceutics and Industrial Pharmacy, Faculty of Pharmacy, Ain Shams University, Cairo, Egypt

[§]Department of Pharmaceutics and Pharmaceutical technology, College of Pharmacy, Taif University, Taif, Kingdom of Saudi Arabia

[∥]School of Physics and Astronomy, Photon Science Institute, University of Manchester, Manchester M13 9PL, United Kingdom

[⊥]School of Biomedicine and School of Materials, Laboratory for Polymers and Biomaterials, University of Manchester, Manchester M13 9PT, United Kingdom

Supporting Information

ABSTRACT: Titania (anatase) nanoparticles were successfully PEGylated through the use of catechol (dopamine)-terminated PEG derivatives. The resulting materials were characterized by excellent stability at neutral pH and extremely low toxicity (phagocytic and nonphagocytic cell lines). In particular, we focused on the comparison between mono- and bis-catechol PEGs. Due to the double terminal anchorage on the titania surface, bis-catechol ligands can produce chains differing from classical monoanchored PEG in conformation (horseshoe-shaped vs brush) and thus the possibility of interactions with biomolecules. At the same time, less than quantitative catechol binding may lead to the presence of dangling chains with unbound catechols which can polymerize and eventually produce PEG/titania nanocomposite colloids. Our results on double-functional PEG2000 show the latter to be the case. Pluronic F127 was also used as a bifunctional ligand, leading to nanocomposite aggregates with an even larger organic content.

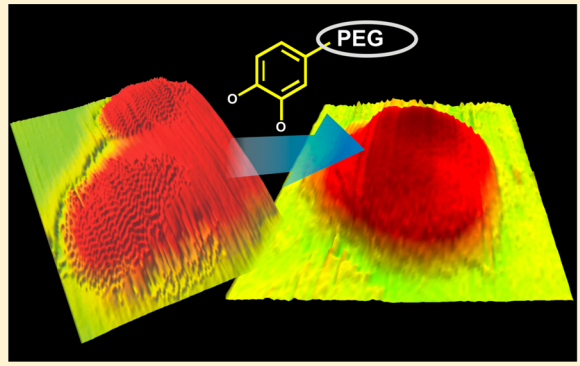

INTRODUCTION

Nanocrystalline titanium dioxide is widely used with applications including cosmetics, paints, and healthcare.[1−3] This versatility is due to its unique optical and chemical properties (high refractive index,[4,5] radio-opacity,[6,7] strong absorption of ultraviolet radiation,[4,5] photoactivity[4,5,8]) together with being inexpensive and easy to prepare in stable suspensions.[9]

Application of TiO_2 nanoparticles in biomedicine has attracted growing attention in the past decade. Originally used as photocatalytic disinfectants under ultraviolet (UV) radiation,[10] TiO_2 nanoparticles have recently been investigated as potential photosensitizing agents for photodynamic therapy (PDT) with the aim of targeting malignant cells in vivo.[11,12] It is well established that these nanoparticles, upon exposure to UV light, trigger formation of reactive oxygen species (ROS) which induce oxidative DNA damage and lipid peroxidation in vitro and in vivo and therefore lead to cell toxicity and death.[11,13,14] It has also been suggested that nanocrystalline TiO_2 can catalyze formation of radical species even in the absence of irradiation[5,15] or by ultrasound activation,[16] correspondingly showing nonphotocatalyic anticancer effects.[11] An additional advantage of TiO_2 is its radio-opacity, and titania nanoparticles can potentially be used as labels for X-ray bioimaging applications.[7]

In an earlier work, we successfully developed a nonaqueous synthesis of ligand-free ("naked") anatase nanoparticles.[17] The nonaqueous process allows for good control of crystal growth also in the absence of surfactants, yielding highly crystalline particles covered by hydrophobic titanium alkoxide surface groups. The latter can be easily hydrolyzed to provide "naked" nanoparticles, which can be then functionalized with a variety of organic ligands.

The importance of control over the surface composition and thus over the aggregation behavior of TiO_2 nanoparticles has often been underestimated; biological evaluation of "naked" titania has been the subject of a number of studies,[5,13] but limited attention has been paid to their colloidal stability in cell

Received: March 29, 2012
Revised: July 2, 2012
Published: July 2, 2012

Scheme 1. Synthesis of the PEGylated Catechols Used in This Study, and Scheme of Their Possible Assemblies on the Surface of Titania Nanoparticles

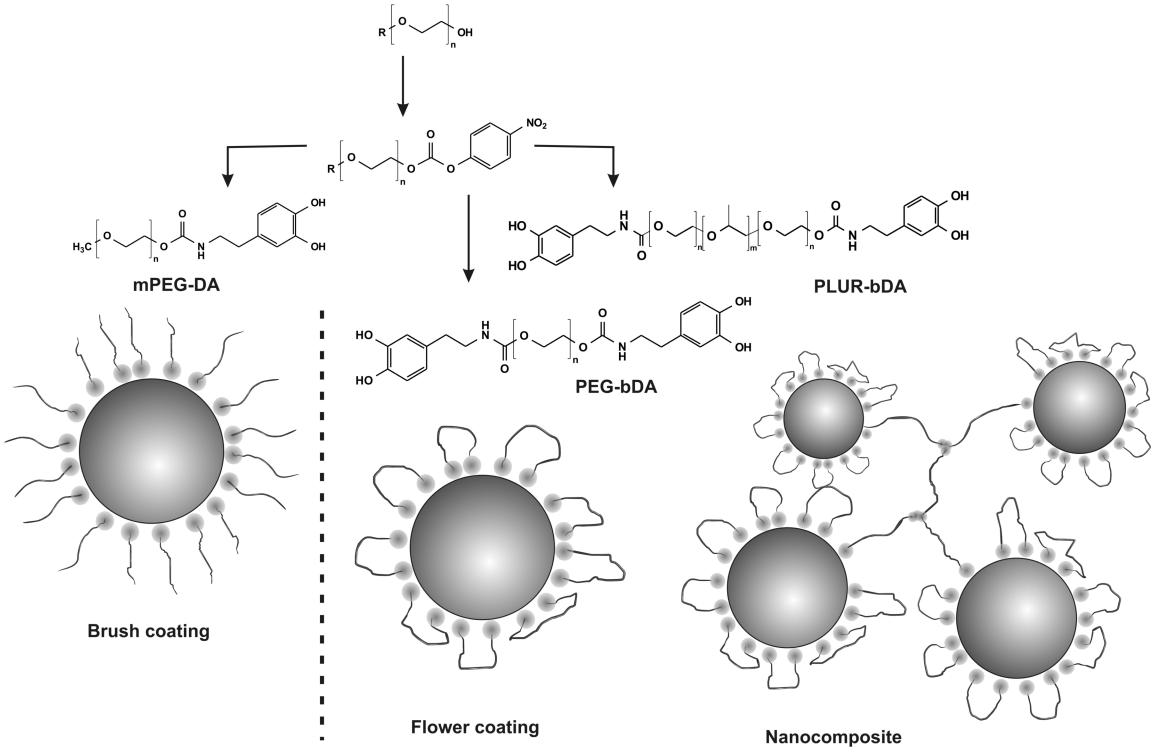

culture media. It is worth pointing out that even simply the use of a neutral pH may be critical, due to its proximity of titania's isoelectric point (pH = 5.6 for rutile[18,19] and 5.8 for anatase);[19] but reports on nano- and microparticles often place it even at values comprised between 6 and 7 (fumed titania[20]).

Surface groups conferring steric stabilization, such as oxyethylene chains, may also be useful in view of biomedical applications, since they may additionally reduce the recognition of nanoparticles as foreign bodies by immune (phagocytic) cells. Indeed, the provision of this "stealth" character to nanocarriers is typically achieved by decoration with hydrophilic, protein-repellent poly(ethylene glycol) (PEG)-based structures,[21,22] which confer prolonged circulation in body fluids, thus enhancing cell/tissue targeting.

PEGylation of titania nanoparticles, however, has not been widely studied. The few examples mostly feature a preliminary functionalization of the titania surface followed by PEGylation reaction, e.g., via surface-initiated atom transfer radical polymerization (ATRP) of PEG-containing monomers,[23] reductive amination,[24] or native chemical ligation;[25] we are aware of only one report of the use of PEG-based ligands (in this case, a salicylic acid derivative).[26]

PEGylation of macroscopic titania surfaces has been more widely investigated; although adsorption of PEG-grafted polyelectrolytes[27] has shown success, use of PEG terminated with catechol groups such as 3,4-dihydroxyphenylalanine (DOPA),[28] anachelin, and dopamine[29] has probably enjoyed more popularity, due to both its efficiency and its biomimetic character: marine mussels are known to secrete catechol-containing proteins to enhance their underwater adhesion to inorganic and organic substrates.[30] Adsorption of low molecular weight catechols onto colloidal TiO_2 has also been extensively studied,[17,31,32] in particular, investigating their influence on nanoparticle optical properties[33] and photoactivity[34] but also the means to confer selective reactivity, e.g., via initiation of surface ATRP.[35]

Here, we applied the catechol-mediated approach to the PEGylation of titania nanoparticles using *p*-nitrophenyl carbonates for introduction of terminal dopamine (DA) groups (Scheme 1). In particular, we focused on the possible outcomes of the use of bifunctional reagents, comparing the effects of the surface adsorption of mono- and bifunctional PEG with identical molecular weight (mPEG-DA and PEG-bDA, respectively) using also Pluronic F127 as a bifunctional ligand with the additional features of larger size and presence of a hydrophobic domain.

Double anchoring could force the macromolecular chain to adopt an overall horseshoe-like morphology (flower coating, as opposed to brush coating, see Scheme 1), which can be characterized by significantly different interactions with biomolecules.[36]

On the other hand, the crowding and reciprocal steric hindrance may not allow all catechols to approach the surface; it is known that catechols are not easily oxidized in the titania-bound form,[37] but in a free form they can easily oligo- and polymerize through their oxidative conversion to quinonic species.[38−40] Therefore, bifunctional ligands adsorbed at one end may be prone to react with similar groups on other particles or with molecules in solution, effectively creating an interparticle matrix and providing a nanocomposite colloid. This different morphology may be beneficial in terms of "stealth" character but may also compromise control over nanoparticle dimensions.

This research aims therefore to study the use of PEGylated catechols to coat "naked" titania nanoparticles, highlighting possible differences in the mode of adsorption between mono- and bifunctional ligands, to ascertain the likelihood of formation of a nanocomposite vs coated particle in the second

dx.doi.org/10.1021/la3012958 | *Langmuir* 2012, 28, 11490−11501

case, and to perform a preliminary toxicity evaluation of the corresponding materials.

MATERIALS AND METHODS

Materials. Benzyl alcohol (anhydrous, 99.8%), titanium(IV) chloride (≥99.0%), triethylamine (≥99%), 4-nitrophenyl chloroformate (96%), dopamine hydrochloride (≥98%), poly(ethylene glycol) diol ($M_n \approx$ 2000 g/mol), poly(ethylene glycol) methyl ether ($M_n \approx$ 2000 g/mol), Pluronic F127 ($M_n \approx$ 12 600), and 0.1 N hydrochloric acid were supplied by Sigma-Aldrich (Buchs, Switzerland). Ethanol (>99.7%) and diethyl ether were purchased from BDH (U.K.). The boric acid gel (3-aminophenylboronic acid polymer bound, particle size 0.1−0.4 mm, boron content 1.4 wt % (dry mass)) was supplied by Sigma-Aldrich (Buchs, Switzerland); in a typical activation procedure, 1−2 g of boric acid gel was swollen in deionized water overnight and successively washed with 1 M HCl, water, 0.1 M NaOH, and finally again deionized water. Water was predistilled and further purified by a Milli-Q system (Millipore, U.K.).

Physico-Chemical Characterization. ^{1}H NMR spectra were recorded on 1% wt $CDCl_3$ and D_2O solutions on a 500 MHz Bruker spectrometer.

Attenuated Total Reflection Infrared Spectroscopy (ATR-IR). FT-IR spectra were recorded in ATR mode on a Tensor 27 Bruker spectrometer. Polymer samples were freeze dried prior to analysis, and TiO_2−polymer water suspensions were evaporated on a heated ATR plate at a temperature of 90 °C. Spectra of the coated nanoparticles were normalized in relation to the peak at 2882 cm^{-1} (ν_{as} CH_2) .

Dynamic Light Scattering (DLS) Analysis and ζ-Potential Measurements. DLS analysis and ζ-potential measurements were performed through a Zetasizer Nano ZS Instrument (Malvern Instrument Ltd., U.K.), with backscattered light detection (173° detection optics) and a 633 nm HeNe laser beam. A Malvern autotitrator MPT-2 was used for measurements at variable pH.

Thermogravimetric Analysis (TGA). About 10 mg of freeze-dried TiO_2 nanoparticle samples was analyzed on a Q5000IR TGA thermobalance (TA Instruments). Analysis was carried out in an inert nitrogen atmosphere with a flow rate of 25 mL min^{-1} and a heating rate of 20 °C min^{-1} with an isotherm at 120 °C (for 60 min or more) in order to quantify the amount of physisorbed water.

X-ray Photoelectron Spectroscopy (XPS). Functionalized nanoparticles were analyzed by XPS using the 300 mm mean radius Scienta analyzer and monochromated Al Kα X-ray source ($h\nu$ = 1486.6 eV) on the ESCA 300 system at the STFC, NCESS facility based at Daresbury Laboratory. Samples were prepared by dropping the nanoparticles dispersed in water onto ITO-coated conducting glass substrates. Substrates were cleaned in an ultrasonic bath prior to the samples being deposited. Samples were allowed to dry in air and then placed in the fast entry lock of the system, and the pressure was allowed to fall below 1 × 10^{-5} mbar before being transferred to the analysis chamber. All spectra were recorded at a near normal take off angle, allowing the maximum sampling depth of the surface.

Atomic Force Microscopy (AFM). AFM analysis was performed using an MFP-3D microscope (Asylum Research, Santa Barbara, CA). A water dispersion of titania nanoparticles was deposited on mica, dried at room temperature under atmospheric pressure, and analyzed in tapping mode with an Olympus AC240TS cantilever (small spring constant-type silicon probe).

UV−Vis Analysis. Adsorption of catechol-bearing ligands onto TiO_2 nanoparticles was monitored by UV−vis spectrophotometry using a Perkin-Elmer Lambda 25 Spectrometer or a Biotek, Synergy 2 plate reader. In a typical experiment performed in a plate reader, absorption spectra were recorded in the spectral range 300−800 nm on 250 μL (corresponding to a path length of 0.78 cm) samples of 0.30 mg/mL suspensions of TiO_2 nanoparticles at pH 1.5 which contained different amounts of catechol-based ligands (concentration of catechol groups 0−3.5 mmol/L). Spectra are assumed to reflect the chemical equilibrium situation, since they were recorded after stabilization of the absorbance at 430−435 nm. The scattering component of the optical density was removed by subtracting a simple exponential baseline from the spectra, as described in a previous work.[17]

Langmuir Balance. A 150 μL amount of coated TiO_2 suspensions (3.5% wt in water) were diluted in 500 μL of ethanol and dialyzed in pure ethanol using regenerated cellulose membrane (15 kDa MWCO). Different volumes of suspension (50−100 μL) were spread at the air/water interface in a Lauda FW2 (Lauda-Königshofen, Germany) Langmuir balance with a maximal interfacial area of 927 cm^2. Surface pressure−area isotherms were recorded at room temperature at a monolayer compression rate of about 40 cm^2/min.

Preparative Procedures. *Synthesis of Catechol-Bearing Polymers. Synthesis of p-Nitrophenyl Carbonate (pNP) Derivatives.* Five mmoles of polymer (poly(ethylene glycol) (PEG), poly(ethylene glycol) methyl ether (mPEG), or Pluronic F127) were dissolved in toluene (200 mL for PEG and mPEG; 350 mL for Pluronic F127) under an inert atmosphere and dried by refluxing the solvent through a Soxhlet extractor filled with activated molecular sieves. After 3 h, the solution was cooled to 0 °C with an ice bath, and 3 equiv (per OH group) of triethylamine (TEA) dissolved in 20 mL of toluene were added. Finally, 2 equiv (per OH group) of 4-nitrophenyl chloroformate (NiP) dissolved in 20 mL of toluene were added dropwise into the reactor, producing a flocculated suspension; the reaction mixture was then stirred at room temperature overnight. The triethylammonium salt was removed by filtration, and solvent was evaporated at a rotary evaporator, yielding a viscous liquid that was diluted with 20 mL of dichloromethane and precipitated in 200 mL of cold diethyl ether. Precipitate was redissolved in 50 mL of dichloromethane, and the precipitation procedure was repeated twice, yielding a light yellow solid, which was stored under inert atmosphere. Yield: 82 ± 4%. Conversion: 95 ± 5 mol %.

^{1}H NMR ($CDCl_3$, ppm). PEG-pNP: δ = 3.6 (m, O−C**H$_2$**−C**H$_2$**−O), 3.8 (t, 2H, PEG−C**H$_2$**−CH$_2$−OC(=O)O), 4.4 (t, 2H, PEG−CH$_2$−C**H$_2$**−OC(=O)O), 7.4 (d, 2H, nitrophenol −CH in ortho to phenol), 8.3 (d, 2H, nitrophenol −CH in ortho to nitro group). mPEG-pNP: δ = 3.4 (s, 3H, O−**CH$_3$**), 3.6 (m, O−**CH$_2$**−**CH$_2$**−O), 3.8 (t, 2H, PEG−C**H$_2$**−CH$_2$−O−), 4.4 (t, 2H PEG−CH$_2$−C**H$_2$**−OC(=O)O), 7.4 (d, 2H, nitrophenol −CH in ortho to phenol), 8.3 (d, 2H, nitrophenol −CH in ortho to nitro group). Pluronic-pNP: δ = 1.1 (d, 3H, O−CH(−**CH$_3$**)−CH$_2$), 3.4 (m, C**H$_2$**−CH−O), 3.5 (m, CH$_2$−C**H**−O), 3.6 (m, O−**CH$_2$**−**CH$_2$**−O), 4.4 (t, 2H −C**H$_2$**−OCOO−), 7.4 (d, 2H, nitrophenol −CH in ortho to phenol), 8.3 (d, 2H, nitrophenol −CH in ortho to nitro group).

ATR-IR (thin film, cm^{-1}). PEG-bpNP: 2990−2790 (ν C−H), 1767 (ν C=O), 1617 (C−C ring stretch), 1528 (NO_2), 1345, 1223, 1107 (ν_{as} C−O−C), 964, 842 (ν_s C−O−C). mPEG-pNP: 2990−2790 (ν C−H), 1766 (ν C=O), 1464 (δ_s CH_2), 1339, 1277, 1238, 1097 (ν_{as} C−O−C), 964 and 842 (ν_s C−O−C). Pluronic-bpNP: 3026 (aromatic ν C−H), 2990−2790 (ν C−H), 1770 (carbonate ν C=O), 1616 and 1593 (C−C ring stretch), 1528 (asymmetric ν NO_2 in $ArNO_2$), 1344, 1281, 1242, 1103 (ν_{as} C−O−C), 948, 842 (ν_s C−O−C).

Reaction of pNP Derivatives with Dopamine. Two equivalents (per pNiP group) of dopamine hydrochloride and 5 equiv (per pNiP group) of TEA were dissolved under inert atmosphere in 50 mL of *N*,*N*-dimethylformamide (DMF). A 5.0 g amount of pNP derivatives was separately dissolved in 50 mL of DMF and subsequently added into the reactor. The reaction mixture was allowed to react for 3 h; DMF was then evaporated at the rotary evaporator (60 °C, 15 mbar), and the resulting viscous oil was purified by precipitation in diethyl ether as described above. The product was then dissolved at a concentration of 2.5% wt in water and transferred in a dialysis membrane with a pore cut off of 1000 g/mol. Yield: 80 ± 2% wt. Conversion: 95 ± 5% mol.

^{1}H NMR (D_2O, ppm). PEG-bDA: δ = 2.7 (t, 4H, Ar−CH$_2$−C**H$_2$**−NH), 3.3 (t, 4H, Ar−C**H$_2$**−CH$_2$−NH), 3.7 (m, O−C**H$_2$**−C**H$_2$**−O), 6.7 (d, 2H, aromatic proton in position 6), 6.8 (s, 2H, aromatic proton in position 2), 6.9 (d, 2H, proton in position 5). mPEG-DA: δ = 2.7 (t, 2H, Ar−CH$_2$−C**H$_2$**−NH), 3.3 (t, Ar−C**H$_2$**−CH$_2$−NH), 3.4 (s, 3H, O−**CH$_3$**), 3.7 (m, O−C**H$_2$**−C**H$_2$**−O), 6.7 (d, 1H, aromatic proton in position 6), 6.8 (s, 1H, aromatic proton in position 2), 6.9 (d, 1H,

dx.doi.org/10.1021/la3012958 | Langmuir 2012, 28, 11490−11501

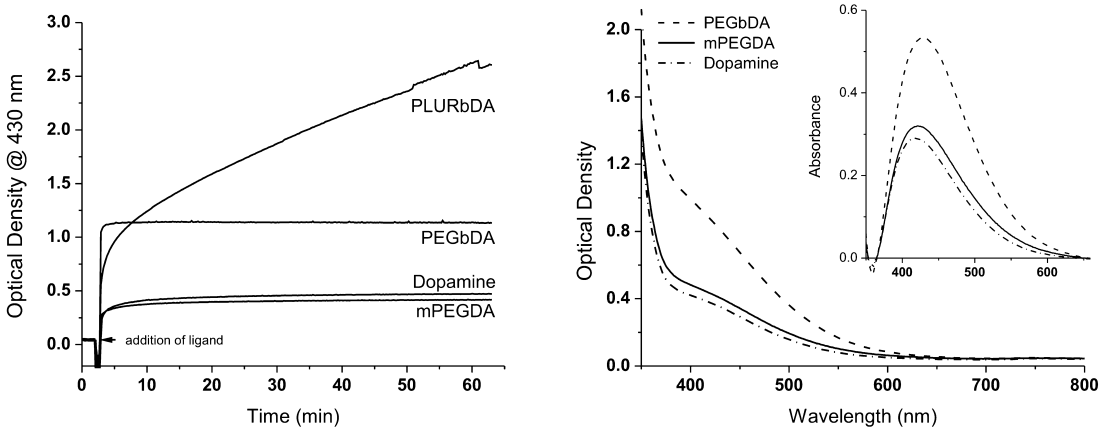

Figure 1. (Left) Absorbance at 430 nm as a function of time for adsorption of ligands onto anatase nanoparticles using concentrations (0.58 mM of catechol and 0.37% wt. titania) far from the saturation of the titania surface (see also Figure 2). Experiments were conducted at pH = 1.5 and room temperature for all samples, with the exception of the PLUR-bDA system, which was used at 10 °C to avoid Pluronic aggregation. (Right) UV−vis spectra of the corresponding systems were recorded 10 min after addition of ligand; (inset) absorption spectra obtained through subtraction of a scattering baseline.

aromatic proton in position 5). PLUR-bDA: δ = 1.2 (d, 3H, C−C**H**$_3$), 2.7 (t, 2H, Ar−CH$_2$−C**H**$_2$−NH), 3.3 (t, Ar−C**H**$_2$−CH$_2$−NH), 3.5 (m, C**H**$_2$−CH−O), 3.6 (m, CH$_2$−C**H**−O), 3.7 (m, O−**CH**$_2$−**CH**$_2$−O), 6.7 (d, 1H, aromatic proton in position 6), 6.8 (s, 1H, aromatic proton in position 2), 6.9 (d, 1H, aromatic proton in position 5) .

ATR-IR (thin film, cm^{-1}). PEG-bDA: 3100−3400 (ν OH), 2882 (ν_{as} CH$_2$), 1713 (ν C═O), 1518 (ω NH), 1104 (ν_{as} C−O−C), 842 (ω aromatic CH). mPEG-DA: 3100−3400 (ν OH), 2882 (ν_{as} CH$_2$), 1714 (ν C═O), 1520 (ω NH), 1098 (ν_{as} C−O−C), 841 (ω aromatic CH). PLUR-bDA: 3100−3400 (ν OH), 2885 (ν_{as} CH$_2$), 1719 (ν C═O), 1516 (ω NH), 1096 (ν_{as} C−O−C), 842 (ω aromatic CH).

Preparation of Anatase Nanoparticles. "Naked" Nanoparticles. A 1 mL amount of TiCl$_4$ (9.12 × 10^{-3} mol of Ti) was introduced dropwise into a glass vial containing 5 mL of anhydrous ethanol, producing a transparent, slightly yellow solution. A 20 mL amount of anhydrous benzyl alcohol (0.19 mols) was added, and the mixture was brought to 80 °C with the container open to air under continuous stirring. The average size of the nanoparticles was measured (DLS in benzyl alcohol) at regular intervals. After 9−10 h objects sized 8−9 nm could be recorded, and correspondingly the suspension turned slightly opaque; at this point the reaction was interrupted, the suspension was precipitated in 80 mL of diethyl ether and centrifuged (3500 rpm for 5 min), and the white precipitate was separated by decantation, washed with diethyl ether, and centrifuged again. The precipitate was then redispersed in 20 mL of 1:1 water−ethanol adjusted to pH = 1.5 using a 0.1 M HCl solution. The resulting suspension was dialyzed in deionized water at pH = 1.5 (HCl) using cellulose ester dialysis membranes (Spectrapore RC) with a molecular weight cut off (MWCO) = 100 000 g/mol. Typically, the final concentration of the suspensions was in the proximity of 1% wt (measured by freeze drying 1 mL of sample and weighing the solid at the end of the process) .

Coated Nanoparticles. In a typical experiment, a polymer solution (0.117 M in catechol groups) in deionized water at pH = 1.5 (HCl) was added to a 0.185% wt suspension of "naked" TiO$_2$ in deionized water at pH =1.5 (HCl), reaching a ratio of 2.53 × 10^{-6} mol of catechol per mg of TiO$_2$. Addition was carried out at room temperature for 5 min for all catechol derivatives (see Figure 1, the equilibrium was reached well before 5 min), except for PLUR-bDA, which was adsorbed for 1 min at 0 °C in order to avoid aggregation. Particles were then purified from nonadsorbed polymers using boric acid gels, which would retain components with free catechol groups. In a 1.5 mL centrifuge tube, 170 mg of activated boric acid gel was swollen under shaking for 5 min in 0.7 mL of sodium carbonate bicarbonate buffer (10% v/v 0.1 M sodium carbonate and 90% 0.1 M sodium bicarbonate, pH 8.5); after addition of 0.35 mL of nanoparticle suspension at pH = 1.5, the centrifuge tube was shaken for 2−3 min and then centrifuged at 10 000 rpm for another 3 min. The supernatant was collected, and the gel was washed again with deionized water to yield a final particle concentration of about 0.50 mg/mL. Higher concentrations could be obtained (e.g., for cytotoxicity testing) via slow evaporation of water at the rotary evaporator. For long-term storage, the nanoparticles were freeze dried in the presence of a cryoprotectant, typically sucrose at a final concentration of 0.5% wt. Resuspension in deionized water followed by dialysis (MWCO = 10 000 Da) did not affect the size distribution of the nanoparticles.

Cytotoxicity Tests. The cytotoxicity of coated nanparticles was tested on murine fibroblasts L929 and macrophages J774.2 (ECACC, U.K.) using the MTT assay (conversion of yellow tetrazolium salt, 3-(4,5-dimethylthiazol-2-yl)-3,5-diphenyl tetrazolium bromide dye (MTT) into highly colored formazan product by mitochondrial reductase enzymes). Both cell lines were cultured in Dulbecco's Modified Eagle's Medium (DMEM) supplemented with 2 mM glutamine and 10% fetal bovine serum (FBS). Cells were split, diluted to 1 × 10^6 cell/mL in culture medium, and seeded in a 96-well plate at a density of 8000 cells/well per 100 μL of culture medium. After incubation for 3 h to allow attachment, the medium was removed by suction and replaced with 100 μL of titania nanoparticles suspensions in complete culture medium at pH 7.4 at a nanoparticle concentration varied between 0.1 and 30 mg/mL. After further 24 h of incubation, the nanoparticle suspension was removed by suction and the cells were washed three times with prewarmed PBS 10 mM pH 7.4. A 100 μL amount of 0.5 mg/mL MTT dissolved in culture medium was added to each well, and incubation followed for 4 h. The stain was removed gently by suction, and the wells were shaken for 5 min in the presence of 100 μL of DMSO in order to solubilize the formazan crystals formed. Viability of the cells was calculated by measuring the absorbance at 550 nm in a plate reader.

RESULTS AND DISCUSSION

Synthesis of Ligands. Catechol-terminated methoxy poly(ethylene glycol) (mPEG-DA; $M_n \approx$ 2000 g/mol), poly(ethylene glycol) diol (PEG-bDA; $M_n \approx$ 2000 g/mol), and Pluronic F127 (PLUR-bDA; $M_n \approx$ 13 000 g/mol, each terminal PEG block; $M_n \approx$ 4000 g/mol) were synthesized through conversion of terminal OH groups to *p*-nitrophenylcarbonates and their successive reaction with the primary amine of dopamine to yield a hydrolytically stable urethane linkage (Scheme 1). Several other groups have reported the use of L-DOPA as a catechol anchor.[28,41] Here, we preferred dopamine, which in its urethane form is neutral throughout a wide pH range, allowing colloidal stabilization of purely steric

dx.doi.org/10.1021/la3012958 | *Langmuir* 2012, 28, 11490−11501

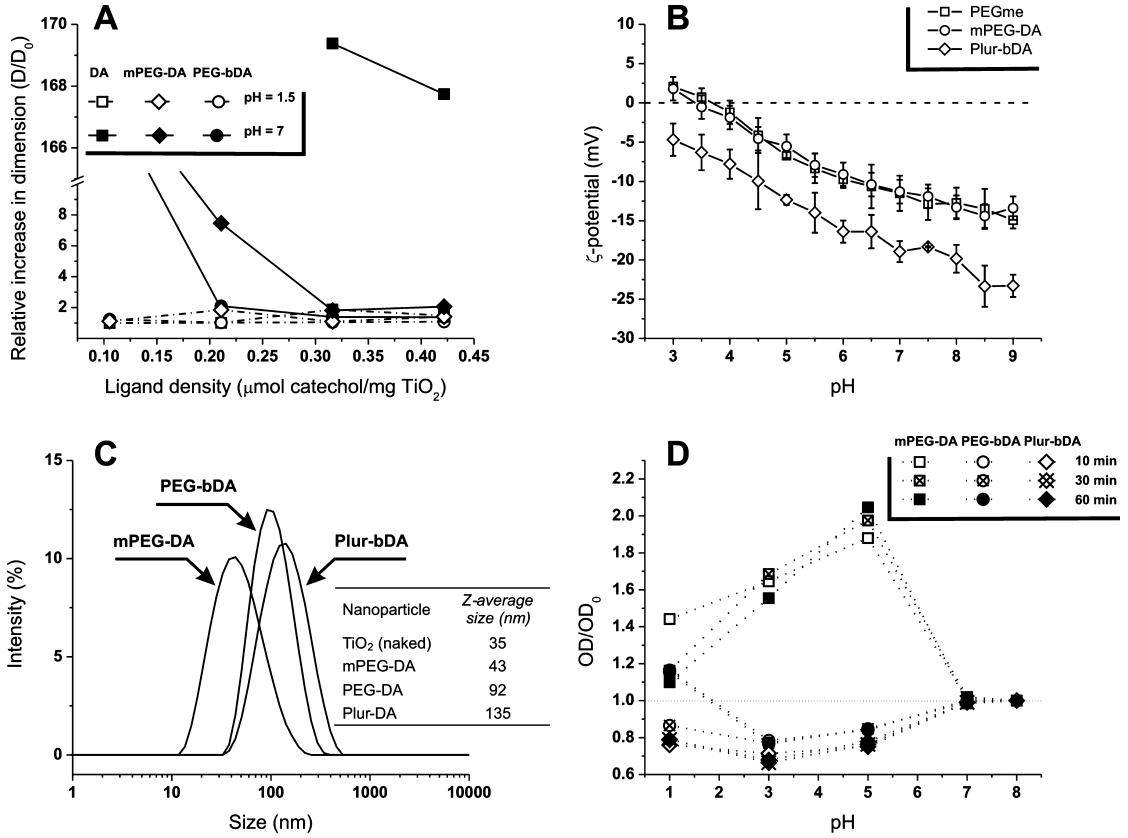

Figure 3. (A) Effect of grafting density (μmol of ligand per mg of TiO_2) on the nanoparticle stability (expressed as a ratio between the average particle size of TiO_2 nanoparticles before and after ligand adsorption) at pH 1.5 and 7. (B) ζ-Potential vs pH for TiO_2 nanoparticles coated with DA-grafted polymers. Nanoparticles were coated with 2.5×10^{-6} mol of catechols per mg of TiO_2, which exceeds the minimum amount to reach the maximum ligand density; free catechols were then removed with a boronic acid gel, which is able to form stable bonds with unreacted dopamine groups under slightly alkaline conditions.[43,44] (C) Size distribution and Z-average size of the coated nanoparticles at neutral pH in deionized water. (D) Optical density at 430 nm (expressed by the ratio OD/OD_0, where OD_0 is the optical density at pH = 8) as a function of pH and storage for different polymer-grafted nanoparticle suspensions.

nature, devoid of any pH-dependent electrostatic contribution to be obtained.

Analysis of Adsorption Behavior. Adsorption of catechol-bearing ligands on anatase nanoparticles (Z-average size = 35 nm; clusters formed by partial aggregation of 8−9 nm nanoparticles, which took place during purification[17]) was studied at pH = 1.5; anatase nanoparticles aggregate extensively at higher pH values. As demonstrated elsewhere,[17] the 400−500 nm spectral window is able to closely monitor the adsorption of catechols on anatase (development of a deep red-orange color). According to the literature,[3] under acidic conditions two concurrent adsorption equilibria occur: catechols may act as chelating agents (two OH on one titanium atom) or be "molecularly adsorbed" and possibly bridge neighboring sites (two OH on two different titanium atoms). Only the chelated form is supposed to produce bands in the visible region of the spectrum;[17] for a given catechol, under the assumption that the ratio between chelating and bridging adsorption is roughly constant, the absorbance can be considered linearly proportional to the overall amount of adsorbed ligands. The optical density in this spectral region increased instantaneously to a plateau level upon addition of dopamine, mPEG-DA, and PEG-bDA; this indicated that both low MW and macromolecular catechols are readily available for rapid complexation of the anatase surface sites (Figure 1, left). The behavior of PLUR-bDA and PEG-bDA is specifically noteworthy.

PLUR-bDA. After 1 min of exposure to PLUR-bDA, the optical density of the dispersion was similar to that obtained upon adsorption of dopamine or mPEG-DA. However, even when lowering the temperature to 10 °C in order to reduce temperature-triggered Pluronic aggregation phenomena,[42] longer exposure times in the acidic adsorption environment caused significant agglomeration and ultimately sedimentation. We believe that transient aggregation between Pluronic surface micelles may lead to exchange of ligands and thus particle-bridging irreversible aggregation. Due to the presence of a time-dependent scattering, the optical density values could not be reliably fitted, and therefore, these nanoparticles will not be further considered in this section.

PEGbDA. At the same concentrations of catechols and nanoparticles, PEG-bDA showed an optical density roughly three times higher than monofunctional systems (Figure 1, left). This difference is partially due to a higher scattering (see Figure 3C), which is likely caused by an increase in dimensions. However, an almost 2-fold difference can still be seen also after subtraction of a scattering baseline (inset in Figure 1, right). For the following analysis it is worth remembering that only chelated complexes are supposed to significantly contribute to the absorbance in the visible region.[17]

dx.doi.org/10.1021/la3012958 | *Langmuir* 2012, 28, 11490−11501

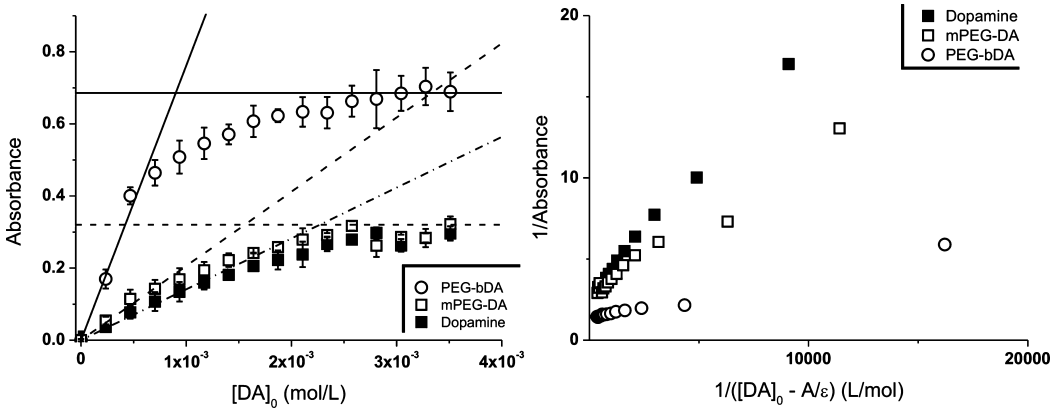

Figure 2. (Left) Optical density at 430 nm recorded 1 min after addition of increasing amounts of catechol-bearing ligand solutions to a 0.3% wt dispersion of "naked" TiO_2 nanoparticles (the appropriate scattering baseline was subtracted from the UV−vis spectra to obtain absorbance values; the latter are here plotted against the total concentration of catechol $[DA]_0$). (Right) Plot of reciprocal of absorbance vs reciprocal of free dopamine concentration.

Table 1. Summary of Adsorption Parameters Calculated from Titration Curves (Figure 2, left)[a]

catechol	$[DA]_{cross}$ (mM)	A_∞	$\varepsilon_{chel}k$ (L/mol)	f_x/f_{DA}[b]	k_x / k_{DA}[c]	K_L (L/mol)
DA	2.1	0.30 ± 0.01	199 ± 5	1	1	2280 ± 220
mPEG-DA	1.5	0.30 ± 0.02	265 ± 15	0.72	1.33	3120 ± 400
PEG-bDA	0.9	0.69 ± 0.05	980 ± 18	0.43	4.9	5074 ± 420

[a]This analysis was not performed with PLUR-bDA as a coating agent due to the rather rapid agglomeration of the nanoparticles. [b]Relative occupancy factor, obtained by dividing the crossover concentration of each catechol by that of dopamine. [c]Relative fraction of catechols in a chelated form, obtained by dividing $\varepsilon_{chel}k$ of each catechol by that of dopamine.

At low total catechol concentration ($[DA]_0 \rightarrow 0$), the absorbance can be expressed as

$$\begin{aligned} A &= \varepsilon_{chel}[TiDA] \\ &= \varepsilon_{chel}k[DA]_{abs} \\ &= \varepsilon_{chel}k([DA]_0 - [DA]_{free}) \end{aligned} \quad (1)$$

where ε_{chel} is the extinction coefficient of the chelated complexes; [TiDA], $[DA]_0$, $[DA]_{ads}$, and $[DA]_{free}$ are, respectively, the concentration of chelated complexes, total catechol, adsorbed catechol, and free catechol in solution; and k is the fraction of catechols adsorbed in chelated complexes. If we assume complexation to be highly favored, the amount of adsorbed catechols can be approximated with the total catechol, i.e., $[DA]_0 - [DA]_{free} \approx [DA]_0$; the initial slope of the adsorption isotherms (Figure 2, left) therefore allows an estimate of the fraction of chelating catechols through the parameter $\varepsilon_{chel}k$. Assuming ε_{chel} to be constant, comparison of the slopes can provide relative values for k.

At high total catechol concentration ($[DA]_0 \rightarrow \infty$), the plateau absorbance is $A_\infty = \varepsilon_{chel}kf[Ti]_0$, where $[Ti]_0$ is the concentration of available titanium sites, which is constant for all experiments, and f is an occupancy factor related to lateral steric hindrance. At a catechol concentration $[DA]_{cross}$ corresponding to the crossover of the two regimes (Figure 2, left: crossing points of the tangents) $A_\infty = \varepsilon_{chel}kf[Ti]_0 \approx \varepsilon_{chel}k[DA]_{cross}$, hence $[DA]_{cross} = [Ti]_0 f$, $[DA]_{cross}$. Therefore, comparison of the catechol concentrations at crossovers can provide a relative estimate of f.

Not surprisingly, the maximum occupancy (f_x/f_{DA} in Table 1) is considerably reduced by conjugation of a PEG chain; it is then dramatically decreased by the PEG double anchoring, which increases the lateral hindrance by not allowing the chain to adopt a brush conformation. Considering the presence of two catechols per chain, a dramatic reduction in the amount of bound PEG-bDA would be expected. The fraction of chelating catechols showed a specular but opposite behavior (k_x/k_{DA} in Table 1): lowest for DA, intermediate for mPEG-DA, and dramatically higher for PEG-bDA, therefore suggesting a very different mode of adsorption for this bifunctional reagent.

For further analysis we employed a Langmuir adsorption model[17]

$$\begin{aligned} [DA]_{abs} &= [DA]_{abs}^{max}\frac{K_L[DA]_{free}}{1 + K_L[DA]_{free}} \\ &= f[Ti]_0\frac{K_L[DA]_{free}}{1 + K_L[DA]_{free}} \end{aligned} \quad (2)$$

where K_L is a Langmuir adsorption constant that is averaged over the to modes of adsorption.

Using eq 1 and considering that $[DA]_{free} = [DA]_0 - [DA]_{abs} = [DA]_0 - A/\varepsilon_{chel}k$, eq 2 can be rearranged as

$$\begin{aligned} \frac{1}{A} &= \frac{1}{\varepsilon_{chel}kf[Ti]_0}\left(1 + \frac{1}{K_L[DA]_{free}}\right) \\ &= \frac{1}{\varepsilon_{chel}kf[Ti]_0}\left(1 + \frac{1}{K_L[DA]_0 - A/\varepsilon_{chel}k}\right) \end{aligned} \quad (3)$$

From the corresponding curves (Figure 2, right), it is finally possible to obtain numerical values for the Langmuir constants (Table 1). For dopamine, the values are analogous to those previously reported;[17] the affinity of mPEG-DA for the titania surface was significantly higher, and again the increase for PEG-bDA was dramatic.

A few conclusions can be drawn.

dx.doi.org/10.1021/la3012958 | Langmuir 2012, 28, 11490−11501

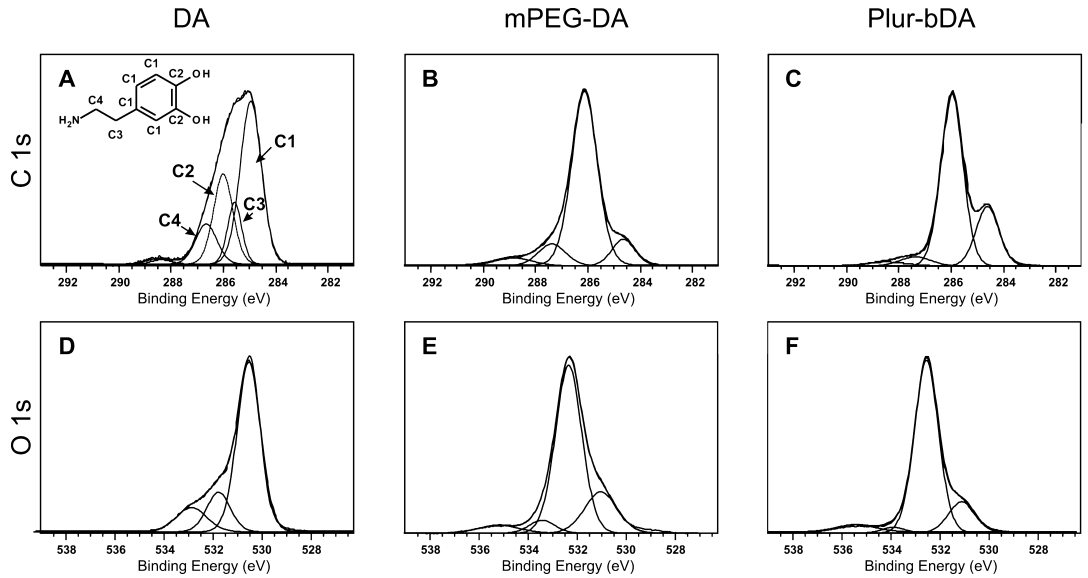

Figure 4. XPS spectra of TiO_2 nanoparticles functionalized with dopamine (TiO_2/DA; (A) C(1s) spectrum, (D) O(1s) spectrum), mPEG-DA (TiO_2/mPEG-DA; (B) C(1s) spectrum, (E) O(1s) spectrum), Plur-bDA (TiO_2/Plur-bDA; (C) C(1s) spectrum, (F) O(1s) spectrum). Detailed summary of all peaks is provided in the Supporting Information, Table 1SI and Table 2SI. Spectra are normalized to the intensity of the strongest peak.

(A) The fraction of chelated complexes appears to grow with the overall affinity in the order DA < mPEG-DA ≪ PEG-bDA. This suggests chelating groups have higher affinity toward titania than bridging ones.

(B) We recorded larger proportions of chelated sites for lower occupancy. It appears therefore that higher steric hindrance may help in the selection of the sites with the highest affinity.

(C) The very high affinity of PEG-bDA may be ascribed to a cooperative effect between the two terminal catechols. Adsorption of one molecule of PEG-bDA would have an overall constant $K = (K_L)^2 = K_1K_2$, where K_1 is the constant for adsorption of the first catechol and K_2 that for the second one. Since K_1 is very likely to be identical to K_L or mPEG-bDA, the second binding constant is $K_2 \geq 10^4$ L/mol.

Size and Stability of Coated Nanoparticles. Adsorption of catechols was performed at pH = 1.5 to ensure the stability of uncoated nanoparticles during the process. At that pH the particle stability against agglomeration did not depend on the ligand density on the nanoparticles (empty symbols, Figure 3A). By increasing the pH to 7 after adsorption (black symbols, Figure 3A) and removing free catechols using a boronic acid gel, macromolecular catechols were shown to provide stability above a density of 3.2×10^{-7} mol per mg of TiO_2; this effect is likely mostly ascribed to steric stabilization, but it is noteworthy that a significantly negative ζ potential was recorded on all systems above pH > 4, with an isoelectric point at pH ≈ 3.5 (Figure 3B). This value is definitely lower than the isoelectric point at pH 5.6 measured with "naked" TiO_2;[17] this decrease is probably due to development of a fractional negative charge on the complexed Ti atoms (as it happens for boronic esters of catechols), while deprotonation of residual free catechols is excluded, since it would happen at higher pH. In a similar study (i.e., adsorption of catechols on TiO_2 nanoparticles), Rodriguez et al. also demonstrated a decrease in surface charge with increasing catechol adsorption and subsequent shift of the isoelectric point to lower pH values.[2]

It is noteworthy that Pluronic-coated nanoparticles showed a significantly more negative ζ potential, which suggests their much larger dimensions (Figure 3C) to be due not only to the higher molecular weight of the polymer but also to the presence of a larger number of catechols, although they may not be all adsorbed on the nanoparticles. DA-coated nanoparticles always produced large aggregates and eventually flocculated, due to the absence of both steric and electrostatic stabilization: at pH = 7 the fractional positive charge of the amine group is possibly compensated by the negative charge seen before.

Compared to their "naked" precursors, all coated TiO_2 nanoparticles increased in size after coating and purification (Figure 3C); the extent of this increase is moderate for TiO_2/mPEG-DA and more pronounced with the use of bifunctional ligands, TiO_2/PEG-bDA and TiO_2/Plur-bDA; the latter effect is likely due to clustering due either to individual ligands directly bridging different particles or to oligomerization of unbound catechol groups creating an interparticle matrix.

The stability of catechol binding to the TiO_2 surface in a physiological range of pH is also a key factor for biological applications. For example, acidic conditions such as those encountered extracellularly in tumor tissues or intracellularly in endolysosomes could cause desorption of catechols; this process may be advantageous, since the resulting aggregation may cause retention at a tumoral site.

Any pH-induced loss of ligands and aggregation of the coated colloids, respectively, would lead to a decrease or an increase of the optical density at 430 nm, which was therefore studied at several pH values for 60 min (Figure 3D). TiO_2/PEG-bDA and TiO_2/Plur-bDA showed a decrease in optical density at acidic pH and no significant agglomeration (DLS) in comparison to neutrality, while TiO_2/mPEG-DA exhibited a large increase, above all at pH = 5, accompanied by visible flocculation. The different behavior could be ascribed to (a) the more difficult desorption of catechols from titania when they are present in a bifunctional structure (cooperative effect) and (b) formation of a nanocomposite structure, which would stabilize the polymers

dx.doi.org/10.1021/la3012958 | *Langmuir* 2012, 28, 11490−11501

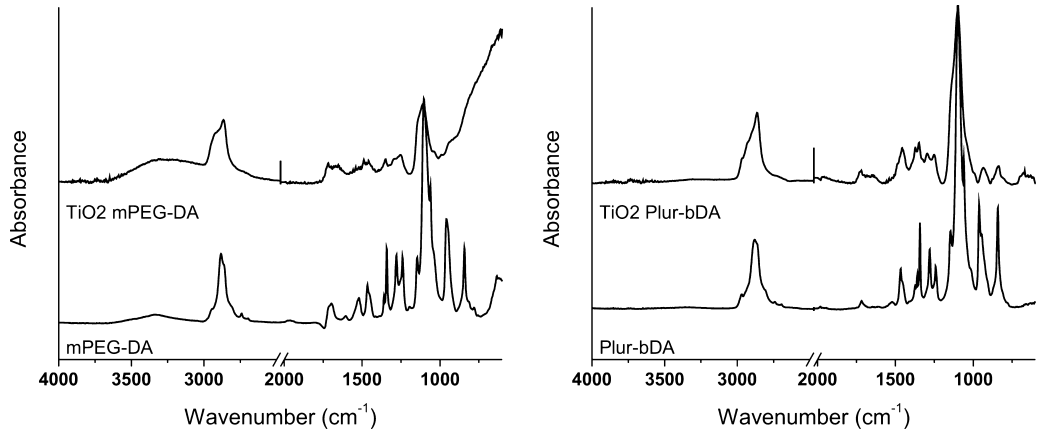

Figure 5. Comparison of the IR spectrum of mPEG-DA with that of mPEG-DA-coated nanoparticles (left) and that of Plur-bDA with that of Plur-bDA coated nanoparticles (right). Spectra for PEG-bDA are analogous to those of mPEG-DA, with a similar presence of titania absorptions below 1000 cm^{-1}.

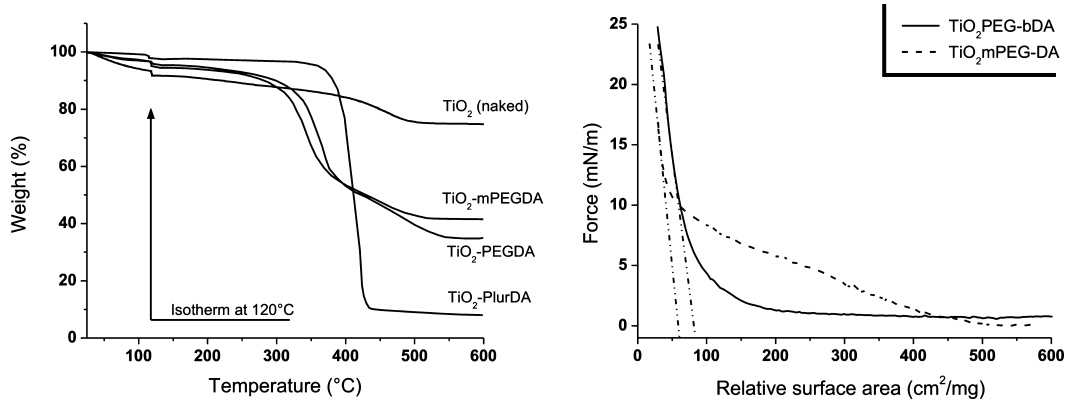

Figure 6. (Left) Thermogravimetric curves of freeze-dried nanoparticles. (Right) Surface pressure vs relative area isotherms of TiO_2/mPEG-DA and TiO_2/PEG-bDA nanoparticles. Isotherms of the TiO_2/Plur-bDA nanoparticles (see Supporting Information, Figure 1SI) are very similar to that of pure Pluronic F127 due to the very small titania content.

around the titania particles possibly through oxidative cross-linking.

Composition and Shape. XPS analysis clearly showed the presence of the catechol ligands. For DA-coated nanoparticles five different peaks can be deconvoluted from the original C(1s) spectrum (Figure 4A). The C1 and C2 peaks at energies of 284.5 and 285.9 eV correspond to the aromatic carbon atoms of the dopamine. The peaks at 285.3 at 286.7 eV correspond to the aliphatic carbon C3 and the primary amine carbon C4, respectively. The peak displaced from the main group is thought to arise from a ring $\pi-\pi^*$ shakeup satellite,[45] and all identified binding energies are in good agreement with those seen in L-DOPA adsorbed on gold.[45] The O 1s band for the same nanoparticles (Figure 4D) showed two main components, at 530.5 and 531.6 eV, which are typically assigned to Ti^{4+}−O and catechol C−O groups, respectively. A third minor band is present at 532.8 eV, which could be related to Ti−OH at the surface.[46,47]

The C 1s spectra recorded from the PEG-coated nanoparticles (see mPEG-DA in Figure 4B as an example) revealed a dominant peak at a binding energy of around 286 eV, which is typical of C−O groups and can be easily assigned to PEG/Pluronic chains; this peak likely includes also the C−O groups of the catechols. A peak at 284.5 eV is also present, which is linked to C1 catechol atoms and to the polymer chain CH_2 groups.[46] The peak at around 287 eV is thought to arise from the C−O bond of the urethane group with a contribution from the C−N bond, while that at 289 eV is attributed to residual carbonates[48] which may not be completely removed from the carbonate−bicarbonate buffer after prolonged dialysis. The O 1s band (Figure 4E) showed a dominant peak at a binding energy of around 532.4 eV which was assigned to the ether oxygen atoms of the polymer chains. The peaks at around 534 and 535 eV arise from traces of carbonate (CO_3^{2-})[48] (due to the use of carbonate/bicarbonate buffer during nanoparticle preparation) and water, respectively.[49] The peak at 531 eV can be attributed to C═O of the urethane anchoring PEG/Pluronic chains to catechols.[50] XPS spectra of Pluronic-coated nanoparticles (Figure 4C and 4F) are similar but show an expected increase in the C 1s peak at 284.5 eV due to the presence of a larger number of C−C bonds (from the poly(propylene glycol block)) and a slight decrease of the O 1s peak associated to the catechol group.

The presence of macromolecular catechols was also confirmed by IR analysis (Figure 5), which showed the presence of all peaks of the precursors also in the coated nanoparticles, with the C−H stretching region (2990−2790 cm^{-1}) and the C−O−C stretching peak (~1100 cm^{-1}) in clear evidence. Most importantly, the Plur-bDA-coated samples showed very little evidence of titania (broad absorption below 1000 cm^{-1}), although peak broadening typical of aggregated samples was recorded.

dx.doi.org/10.1021/la3012958 | Langmuir 2012, 28, 11490−11501

Thermogravimetric analysis (TGA) was used to quantify the amount of organic material present on the nanoparticles after dialysis and freeze drying (Figure 6, left). It is worth pointing out that at neutral pH the catechol adsorption is substantially irreversible and virtually the same amount of organics could be observed independently on the time of dialysis. A first weight loss was observed up to 120 °C, corresponding to removal of physically adsorbed water. Further weight losses observed in the 120−600 °C range corresponded to loss of organic residues and water (condensation of titanols) from the surface of the coated TiO_2. The calculated compositions (Table 2) showed a reduced presence of adsorbed water on coated nanoparticles, which is reasonable due to the lower hydrogen-bonding capacity of PEG in comparison to the freely accessible titanols of the "naked" nanoparticles. The adsorbed water was minimal for TiO_2/Plur-bDA, but the dramatic weight loss at about 400 °C showed these particles to be mostly composed of organic material with very little titania (~10% wt); considering also the IR results and previous observations of size and ζ-potential, it would appear that Plur-bDA was predominantly present in an aggregated form, rather than simply coating the surface of the nanoparticles.

Table 2. Summary of TGA Data for Naked and Coated Titania Nanoparticles

	dry mass %[a]	TiO_2 %[b]	organics %[c]	OH %[d]	organics/TiO_2[e]
TiO_2 (naked)	91.7	73.9	=	17.8	=
TiO_2/mPEG-DA	94.5	41.6	42.5	10.4	1.02
TiO_2/PEG-bDA	95.8	35.0	44.8	16.0	1.28
TiO_2/Plur-bDA	97.8	8.1	89.7	=	11.1

[a]Weight percentage of dry mass remaining after loss of physisorbed water during 1 h of isothermal treatment at 120 °C. [b]Weight percentage of TiO_2, calculated as residual mass present at 600 °C. [c]Weight percentage of organics present on the nanoparticle surface, calculated as weight loss between 120 and 400 °C. [d]Weight percentage of titanols present on the nanoparticle surface, calculated as weight loss between 400 and 600 °C. [e]Weight ratio between the organic fraction (volatile between 120 and 400 °C) and TiO_2 (residue at 600 °C).

Surprisingly, TiO_2/PEG-bDA showed a higher polymer content than TiO_2/mPEG-DA; considering the lower amount of bound PEG estimated from the adsorption data, TiO_2/PEG-bDA appear to have a significant amount of unbound polymer. Uncomplexed catechols may react between themselves and cross-link PEG chains, leading also to nanoparticle aggregation during surface functionalization; this would contribute to explain the higher stability against ligand desorption and the considerably larger size of the TiO_2 /PEG-bDA nanoparticles.

Due to the presence of these excess polymer chains, TiO_2/PEG-bDA nanoparticles should be considerably softer than TiO_2/mPEG-DA ones. To verify this hypothesis we compared their pressure/surface area isotherms at the air−water interface (Figure 6, right). At high lateral pressure, both kinds of nanoparticles showed a similar solid-like behavior; under the assumption of an elastic behavior, the limiting areas at zero pressure are 84 cm^2/g for mPEG-DA nanoparticles and 61 cm^2/g for PEG-bDA ones. Using some rather rough assumptions, we will convert these values in "unperturbed" dimensions per titania core: if difunctional PEG chains creates a matrix surrounding the titania cores in TiO_2/PEG-bDA, rather than more rigidly bridging them, we expect them to have a limiting area per core similar to that of TiO_2/mPEG-DA. First, we will assume the density of "naked" nanoparticles to be the

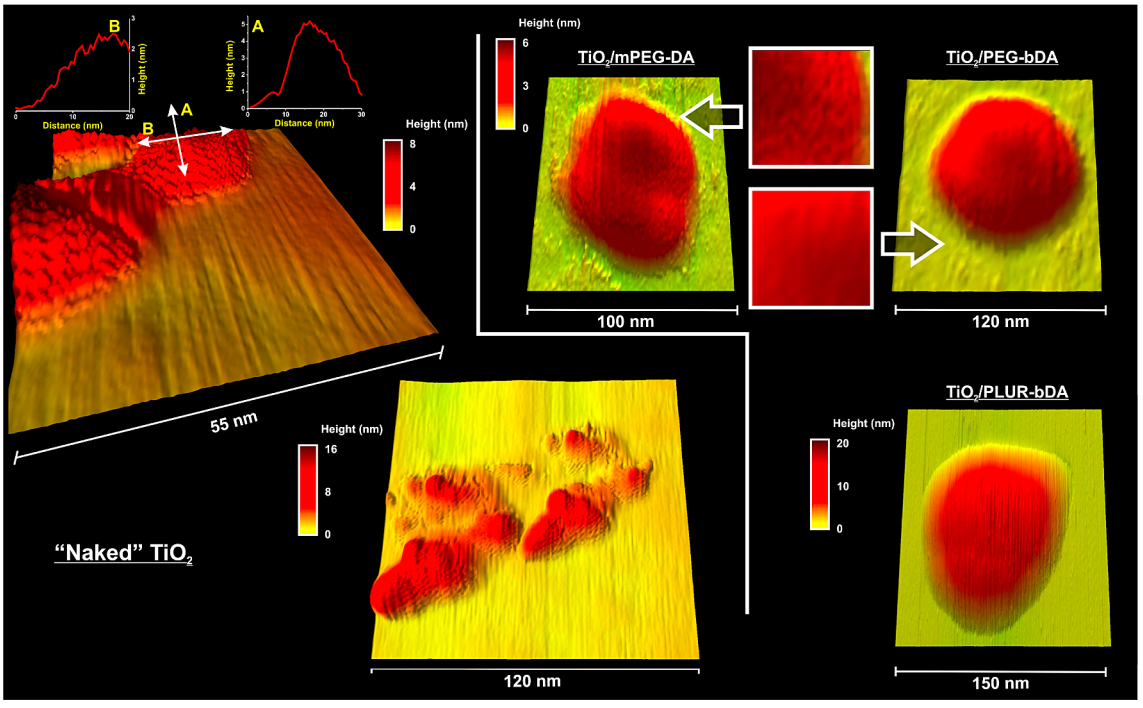

Figure 7. AFM images recorded in tapping mode for nanoparticles deposited on mica from deionized water dispersions). (Left) Uncoated TiO_2 nanoparticles; two insets on the top show the profile of one nanoparticle along two perpendicular directions (white arrows). (Right) Coated nanoparticles; from careful inspection of the images (insets), TiO_2/mPEG-DA nanoparticles show some residual surface roughness, which disappears almost completely in TiO_2/PEG-bDA and is totally absent in TiO_2/Plur-bDA.

dx.doi.org/10.1021/la3012958 | Langmuir 2012, 28, 11490−11501

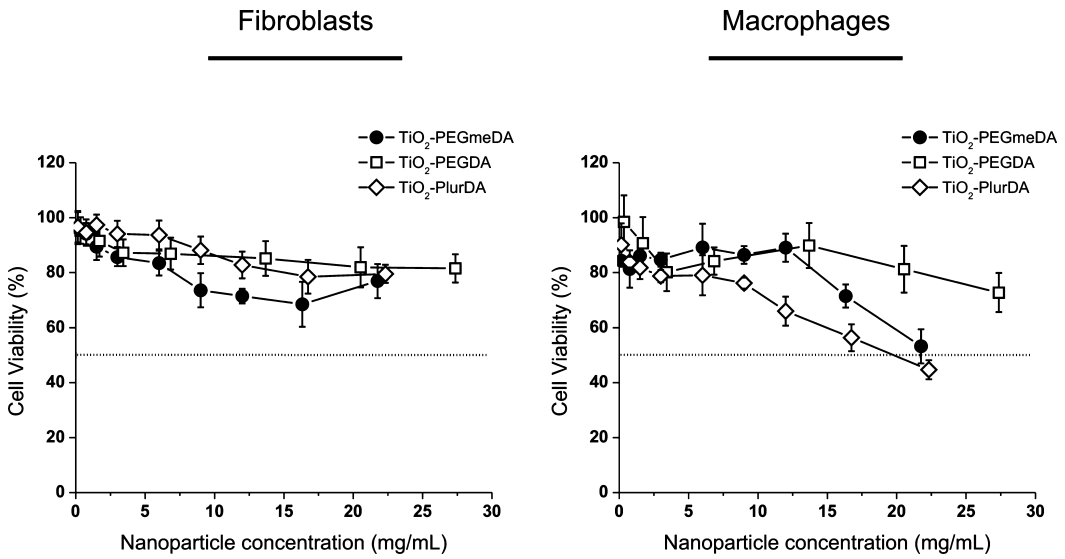

Figure 8. Cell viability (MTT assay) for L929 fibroblasts (left) and J774.2 macrophages (right) as a function of nanoparticle concentration at 37 °C after 24 h exposure.

same as anatase (4.23 g/cm^3): a 35 nm titania core would have a weight of 8.9 × 10^{-14} mg. Considering the titania weight fractions reported in Table 1, this would correspond to a weight of 2.1 × 10^{-13} and 2.5 × 10^{-13} g per coated titania core, respectively, in TiO_2/mPEG-DA and TiO_2/PEG-bDA nanoparticles. Using these values, the above limiting areas would correspond to about 1750 and 1500 nm^2 per particle. This similarity would therefore suggest a rather loose connection between titania cores in TiO_2/PEG-bDA, which is possibly more coherent with cross-linked rather than bridging PEG chains.

On the other hand, at large surface areas TiO_2/PEG-bDA showed disorganized, liquid-like behavior (= gradual increase in pressure), whereas no such effect was noticeable for TiO_2/mPEG-DA.

This apparent biphasic behavior of TiO_2/PEG-bDA would support a composite structure made of titania cores dispersed in aggregated/cross-linked PEG soft domain, which would be consistent with both DLS and TGA data.

We used AFM to compare the different nanoparticles. Once deposited on mica, naked TiO_2 nanoparticles presented an irregular but flattened (typical height 6−8 nm) morphology (Figure 7, left), as previously reported;[17] this is likely due to aggregation of smaller (6−10 nm) individual particles, which appear to have a rather loose internal cohesion. The particles also showed a typical and quite regular surface roughness (typically 0.2−0.3 nm) that suggests direct surface exposure of crystalline phases.

The features of TiO_2/mPEG-DA nanoparticles were coherent with the presence of a PEG monolayer coating the titania aggregates: similar flattened shape (thickness 6−8 nm), but a larger lateral size and a smoother surface, with clear sign of residual regular roughness generally beyond the analytical capacity of AFM (Figure 8, right, see insets). TiO_2/PEG-bDA nanoparticles were larger but with identical height, which indicates the presence of the same kind of hard objects. However, the surface relief was almost completely lost: we speculate that if their larger size was due to PEG-bDA simply bridging different titania cores the roughness would be similar to TiO_2/mPEG-DA; its absence, on the contrary, suggests the titania cores to be embedded in a (soft) matrix. PLUR-bDA-coated nanoparticles showed larger dimensions and an even smoother surface, which is coherent with them being mostly composed of aggregate/cross-linked Pluronic.

Cytotoxicity. The effect of nanoparticles on cell viability was evaluated through the MTT assay on two murine cell lines after a 24 h exposure: J774 macrophages were used as a more sensitive, phagocytic model[51−53] and L929 fibroblasts as a nonphagocytic and widely recommended reference cell line. All nanoparticles are heavily PEGylated, and unsurprinsingly, they were found to have extremely low cytotoxicity (Figure 8): a 50% decrease of viability was recorded only for macrophages exposed to mPEG-DA- and Plur-bDA-coated nanoparticles at concentrations > 2% wt. The slightly lower viability of macrophages exposed to Plur-bDA nanoparticles can probably be ascribed to the detergent and thus membrane-damaging nature of Pluronic F127, which was shown (TGA, IR) to be the overwhelming component of these aggregates.

■ CONCLUSIONS

Use of PEGylated catechols for surface decoration of TiO_2 nanoparticles leads to stable, low-toxicity particles, but has some caveats. First, it is generally true that both mode and strength of adsorption depend on the macromolecular architecture of the ligand; however, bulkier ligands that are adsorbed at lower surface densities due to higher steric hindrance perhaps counterintuitively may have a higher affinity to the surface sites. Additionally, bi- (or multi)dentate ligands appear to unavoidably lead to significant aggregation, generating nanocomposite systems rather than individual core−shell nanoparticles. Aggregation can be produced by bridging of different particles by the ligand, but the larger than expected polymer content and the softer character of the colloids lead us to ascribe the effects to oxidative oligomerization of unbound catechols.

■ ASSOCIATED CONTENT

Ⓢ Supporting Information

Detailed assignment and relative proportions of the XPS C 1s and O 1s peaks of coated nanoparticles; surface pressure vs relative surface area isotherms for TiO_2/Plur-bDA nano-

dx.doi.org/10.1021/la3012958 | Langmuir 2012, 28, 11490−11501

particles. This material is available free of charge via the Internet at http://pubs.acs.org.

AUTHOR INFORMATION

Corresponding Author

*E-mail: f.cellesi@manchester.ac.uk (F.C.); Nicola.tirelli@manchester.ac.uk (N.T.).

Notes

The authors declare no competing financial interest.

ACKNOWLEDGMENTS

Mr. Roberto Donno and Dr. Giona Kilcher are gratefully acknowledged, respectively, for discussions on AFM and help in the synthesis of the polymeric substrates. The National Centre for Electron Spectroscopy and Surface Analysis (NCESSA) was funded by EPSRC(UK) under grant ref EP/E025722/1.

REFERENCES

(1) Giammar, D. E.; Maus, C. J.; Xie, L. Y. Effects of particle size and crystalline phase on lead adsorption to titanium dioxide nanoparticles. *Environ. Eng. Sci.* **2007**, *24* (1), 85−95.

(2) Rodriguez, R.; Blesa, M. A.; Regazzoni, A. E. Surface complexation at the TiO_2 (anatase) aqueous solution interface: Chemisorption of catechol. *J. Colloid Interface Sci.* **1996**, *177* (1), 122−131.

(3) Lana-Villarreal, T.; Rodes, A.; Perez, J. M.; Gomez, R. A spectroscopic and electrochemical approach to the study of the interactions and photoinduced electron transfer between catechol and anatase nanoparticles in aqueous solution. *J. Am. Chem. Soc.* **2005**, *127* (36), 12601−12611.

(4) Jin, C. Y.; Zhu, B. S.; Wang, X. F.; Lu, Q. H. Cytotoxicity of titanium dioxide nanoparticles in mouse fibroblast cells. *Chem. Res. Toxicol.* **2008**, *21* (9), 1871−1877.

(5) Sayes, C. M.; Wahi, R.; Kurian, P. A.; Liu, Y. P.; West, J. L.; Ausman, K. D.; Warheit, D. B.; Colvin, V. L. Correlating nanoscale titania structure with toxicity: A cytotoxicity and inflammatory response study with human dermal fibroblasts and human lung epithelial cells. *Toxicol. Sci.* **2006**, *92* (1), 174−185.

(6) Goto, K.; Tamura, J.; Shinzato, S.; Fujibayashi, S.; Hashimoto, M.; Kawashita, M.; Kokubo, T.; Nakamura, T. Bioactive bone cements containing nano-sized titania particles for use as bone substitutes. *Biomaterials* **2005**, *26* (33), 6496−6505.

(7) Ashcroft, J. M.; Gu, W.; Zhang, T.; Hughes, S. M.; Hartman, K. B.; Hofmann, C.; Kanaras, A. G.; Kilcoyne, D. A.; Le Gros, M.; Yin, Y.; Alivisatos, A. P.; Larabell, C. A. TiO2 nanoparticles as a soft X-ray molecular probe. *Chem. Commun.* **2008**, *21*, 2471−2473.

(8) Hurum, D. C.; Agrios, A. G.; Gray, K. A.; Rajh, T.; Thurnauer, M. C. Explaining the enhanced photocatalytic activity of Degussa P25 mixed-phase TiO2 using EPR. *J. Phys. Chem. B* **2003**, *107* (19), 4545−4549.

(9) Fabian, E.; Landsiedel, R.; Ma-Hock, L.; Wiench, K.; Wohlleben, W.; van Ravenzwaay, B. Tissue distribution and toxicity of intravenously administered titanium dioxide nanoparticles in rats. *Arch. Toxicol.* **2008**, *82* (3), 151−157.

(10) Matsunaga, T.; Tomoda, R.; Nakajima, T.; Wake, H. Photoelectrochemical Sterilization of Microbial-Cells by Semiconductor Powders. *Fems Microbiol. Lett.* **1985**, *29* (1−2), 211−214.

(11) Thevenot, P.; Cho, J.; Wavhal, D.; Timmons, R. B.; Tang, L. P. Surface chemistry influences cancer killing effect of TiO2 nanoparticles. *Nanomed.-Nanotechnol. Biol. Med.* **2008**, *4* (3), 226−236.

(12) Xu, J.; Sun, Y.; Huang, J. J.; Chen, C. M.; Liu, G. Y.; Jiang, Y.; Zhao, Y. M.; Jiang, Z. Y. Photokilling cancer cells using highly cell-specific antibody-TiO2 bioconjugates and electroporation. *Bioelectrochemistry* **2007**, *71* (2), 217−222.

(13) Maness, P. C.; Smolinski, S.; Blake, D. M.; Huang, Z.; Wolfrum, E. J.; Jacoby, W. A. Bactericidal activity of photocatalytic TiO2 reaction: Toward an understanding of its killing mechanism. *Appl. Environ. Microbiol.* **1999**, *65* (9), 4094−4098.

(14) Seo, J.-w.; Chung, H.; Kim, M.-y.; Lee, J.; Choi, I.-h.; Cheon, J. Development of Water-Soluble Single-Crystalline TiO2 Nanoparticles for Photocatalytic Cancer-Cell Treatment. *Small* **2007**, *3* (5), 850−853.

(15) Wang, J. X.; Fan, Y. B.; Gao, Y.; Hu, Q. H.; Wang, T. C. TiO2 nanoparticles translocation and potential toxicological effect in rats after intraarticular injection. *Biomaterials* **2009**, *30* (27), 4590−4600.

(16) Harada, Y.; Ogawa, K.; Irie, Y.; Endo, H.; Feril, L. B.; Uemura, T.; Tachibana, K., Ultrasound activation of TiO2 in melanoma tumors. *J. Controlled Release 149*, (2), 190-195.

(17) Kotsokechagia, T.; Cellesi, F.; Thomas, A.; Niederberger, M.; Tirelli, N. *Preparation of Ligand-Free TiO_2 (Anatase) Nanoparticles through a Nonaqueous Process and Their Surface Functionalization*; 2008; Vol. *24*, pp 6988−6997.

(18) Larson, I.; Drummond, C. J.; Chan, D. Y. C.; Grieser, F. Direct Force Measurements Between TiO_2 surfaces. *J. Am. Chem. Soc.* **1993**, *115* (25), 11885−11890.

(19) Kosmulski, M. The significance of the difference in the point of zero charge between rutile and anatase. *Adv. Colloid Interface Sci.* **2002**, *99* (3), 255−264.

(20) Gun'ko, V. M.; Zarko, V. I.; Leboda, R.; Chibowski, E. Aqueous suspension of fumed oxides: particle size distribution and zeta potential. *Adv. Colloid Interface Sci.* **2001**, *91* (1), 1−112.

(21) Amstad, E.; Zurcher, S.; Mashaghi, A.; Wong, J. Y.; Textor, M.; Reimhult, E. Surface Functionalization of Single Superparamagnetic Iron Oxide Nanoparticles for Targeted Magnetic Resonance Imaging. *Small* **2009**, *5* (11), 1334−1342.

(22) Owens, D. E.; Peppas, N. A. Opsonization, biodistribution, and pharmacokinetics of polymeric nanoparticles. *Int. J. Pharm.* **2006**, *307* (1), 93−102.

(23) Park, J. T.; Koh, J. H.; Koh, J. K.; Kim, J. H. Surface-initiated atom transfer radical polymerization from TiO2 nanoparticles. *Appl. Surf. Sci.* **2009**, *255* (6), 3739−3744.

(24) Vasilev, K.; Poh, Z.; Kant, K.; Chan, J.; Michelmore, A.; Losic, D. Tailoring the surface functionalities of titania nanotube arrays. *Biomaterials* **2010**, *31* (3), 532−540.

(25) Byun, E.; Kim, J.; Kang, S. M.; Lee, H.; Bang, D. Surface PEGylation via Native Chemical Ligation. *Bioconjugate Chem.* **2011**, *22* (1), 4−8.

(26) Yamaguchi, S.; Kobayashi, H.; Narita, T.; Kanehira, K.; Sonezaki, S.; Kubota, Y.; Terasaka, S.; Iwasaki, Y. Novel Photodynamic Therapy Using Water-dispersed TiO(2)-Polyethylene Glycol Compound: Evaluation of Antitumor Effect on Glioma Cells and Spheroids In Vitro. *Photochem. Photobiol.* **2010**, *86* (4), 964−971.

(27) Kenausis, G. L.; Voros, J.; Elbert, D. L.; Huang, N. P.; Hofer, R.; Ruiz-Taylor, L.; Textor, M.; Hubbell, J. A.; Spencer, N. D. Poly(L-lysine)-*g*-poly(ethylene glycol) layers on metal oxide surfaces: Attachment mechanism and effects of polymer architecture on resistance to protein adsorption. *J. Phys. Chem. B* **2000**, *104* (14), 3298−3309.

(28) Dalsin, J. L.; Lin, L. J.; Tosatti, S.; Voros, J.; Textor, M.; Messersmith, P. B. Protein resistance of titanium oxide surfaces modified by biologically inspired mPEG-DOP. *Langmuir* **2005**, *21* (2), 640−646.

(29) Zurcher, S.; Wackerlin, D.; Bethuel, Y.; Malisova, B.; Textor, M.; Tosatti, S.; Gademann, K. Biomimetic Surface Modifications Based on the Cyanobacterial Iron Chelator Anachelin. *J. Am. Chem. Soc.* **2006**, *128* (4), 1064−1065.

(30) Waite, J. H. Natures Underwater Adhesive Specialist. *Int. J. Adhesion Adhesives* **1987**, *7* (1), 9−14.

(31) Creutz, C.; Chou, M. H. Binding of catechols to mononuclear titanium(IV) and to 1-and 5-nm TiO2 nanoparticles. *Inorg. Chem.* **2008**, *47* (9), 3509−3514.

(32) de la Garza, L.; Saponjic, Z. V.; Dimitrijevic, N. M.; Thurnauer, M. C.; Rajh, T. Surface states of titanium dioxide nanoparticles modified with enediol ligands. *J. Phys. Chem. B* **2006**, *110* (2), 680−686.

(33) Jankovic, I. A.; Saponjic, Z. V.; Comor, M. I.; Nedeljlkovic, J. M. Surface Modification of Colloidal TiO2 Nanoparticles with Bidentate Benzene Derivatives. *J. Phys. Chem. C* **2009**, *113* (29), 12645−12652.
(34) Dimitrijevic, N. M.; Rozhkova, E.; Rajh, T. Dynamics of Localized Charges in Dopamine-Modified TiO2 and their Effect on the Formation of Reactive Oxygen Species. *J. Am. Chem. Soc.* **2009**, *131* (8), 2893−2899.
(35) Fan, X. W.; Lin, L. J.; Messersmith, P. B. Surface-initiated polymerization from TiO2 nanoparticle surfaces through a biomimetic initiator: A new route toward polymer-matrix nanocomposites. *Compos. Sci. Technol.* **2006**, *66* (9), 1198−1204.
(36) Chaudhari, K.; Ukawala, M.; Manjappa, A.; Kumar, A.; Mundada, P.; Mishra, A.; Mathur, R.; Mönkkönen, J.; Murthy, R. Opsonization, Biodistribution, Cellular Uptake and Apoptosis Study of PEGylated PBCA Nanoparticle as Potential Drug Delivery Carrier. *Pharm. Res.* **2012**, *29* (1), 53−68.
(37) Rajh, T.; Chen, L. X.; Lukas, K.; Liu, T.; Thurnauer, M. C.; Tiede, D. M. Surface Restructuring of Nanoparticles: An Efficient Route for Ligand-Metal Oxide Crosstalk. *J. Phys. Chem. B* **2002**, *106*, 10543−10552.
(38) Jiang, J. H.; Zhu, L. P.; Zhu, L. J.; Zhu, B. K.; Xu, Y. Y. Surface Characteristics of a Self-Polymerized Dopamine Coating Deposited on Hydrophobic Polymer Films. *Langmuir* **2011**, *27* (23), 14180−14187.
(39) Lee, H.; Dellatore, S. M.; Miller, W. M.; Messersmith, P. B. Mussel-inspired surface chemistry for multifunctional coatings. *Science* **2007**, *318* (5849), 426−430.
(40) Tsai, W. B.; Chen, W. T.; Chien, H. W.; Kuo, W. H.; Wang, M. J. Poly(dopamine) coating of scaffolds for articular cartilage tissue engineering. *Acta Biomater.* **2011**, *7* (12), 4187−4194.
(41) Lee, B. P.; Dalsin, J. L.; Messersmith, P. B. Synthesis and gelation of DOPA-Modified poly(ethylene glycol) hydrogels. *Biomacromolecules* **2002**, *3* (5), 1038−1047.
(42) Cellesi, F.; Tirelli, N.; Hubbell, J. A. Materials for cell encapsulation via a new tandem approach combining reverse thermal gelation and covalent crosslinking. *Macromol. Chem. Phys.* **2002**, *203* (10−11), 1466−1472.
(43) Imai, Y.; Ito, S.; Maruta, K.; Fujita, K. Simultaneous Determination of Catecholamines and Serotonin by Liquid-Chromatography, after Treatment with Boric-Acid Gel. *Clin. Chem.* **1988**, *34* (3), 528−530.
(44) Maruta, K.; Fujita, K.; Ito, S.; Nagatsu, T. Liquid-Chromatography of Plasma-Catecholamines, with Electrochemical Detection, after Treatment with Boric-Acid Gel. *Clin. Chem.* **1984**, *30* (7), 1271−1273.
(45) Weinhold, M.; Soubatch, S.; Temirov, R.; Rohlfing, M.; Jastorff, B.; Tautz, F. S.; Doose, C. Structure and bonding of the multifunctional amino acid L-DOPA on Au(110). *J. Phys. Chem. B* **2006**, *110* (47), 23756−23769.
(46) Huang, N. P.; Michel, R.; Voros, J.; Textor, M.; Hofer, R.; Rossi, A.; Elbert, D. L.; Hubbell, J. A.; Spencer, N. D. Poly(L-lysine)-*g*-poly(ethylene glycol) layers on metal oxide surfaces: Surface-analytical characterization and resistance to serum and fibrinogen adsorption. *Langmuir* **2001**, *17* (2), 489−498.
(47) Syres, K.; Thomas, A.; Bondino, F.; Malvestuto, M.; Gratzel, M. Dopamine Adsorption on Anatase TiO(2)(101): A Photoemission and NEXAFS Spectroscopy Study. *Langmuir* **2010**, *26* (18), 14548−14555.
(48) Fornasiero, D.; Li, F. S.; Ralston, J.; Smart, R. S. C. Oxidation of Galena Surfaces 0.1. X-Ray Photoelectron Spectroscopic and Dissolution Kinetics Studies. *J. Colloid Interface Sci.* **1994**, *164* (2), 333−344.
(49) Russat, J. Characterization of Polyamic Acid Polyimide Films in the Nanometric Thickness Range from Spin-Deposited Polyamic Acid. *Surf. Interface Anal.* **1988**, *11* (8), 414−420.
(50) Jiang, M.; Hu, P. Surface modification of a biomedical poly(ester) urethane by several low-powered gas plasmas. *J. Appl. Polym. Sci.* **2006**, *101* (3), 1273−1282.
(51) Green, T. R.; Fisher, J.; Stone, M.; Wroblewski, B. M.; Ingham, E. Polyethylene particles of a 'critical size' are necessary for the induction of cytokines by macrophages in vitro. *Biomaterials* **1998**, *19* (24), 2297−2302.
(52) Olivier, V.; Rivière, C.; Hindié, M.; Duval, J. L.; Bomila-Koradjim, G.; Nagel, M. D. Uptake of polystyrene beads bearing functional groups by macrophages and fibroblasts. *Colloids Surf., B* **2004**, *33* (1), 23−31.
(53) Zahr, A. S.; Davis, C. A.; Pishko, M. V. Macrophage uptake of core-shell nanoparticles surface modified with poly(ethylene glycol). *Langmuir* **2006**, *22* (19), 8178−85.